

Collective Dynamics of Magnetic Vortices in an Array of Interacting Nanodots

P. D. Kim^a, V. A. Orlov^{b,*}, R. Yu. Rudenko^a, V. S. Prokopenko^b,
I. N. Orlova^b, and S. S. Zamai^c

^a Kirensky Institute of Physics, Siberian Branch, Russian Academy of Sciences,
Akademgorodok, Krasnoyarsk, 660036 Russia

^b Krasnoyarsk State Pedagogical University, ul. Ady Lebedevoi 89, Krasnoyarsk, 660049 Russia

* e-mail: orlhome@rambler.ru

^c Krasnoyarsk State Medical University, Krasnoyarsk, 660022 Russia

Received March 11, 2015; in final form, March 18, 2015

The lift of the degeneracy of the resonance frequency of motion of the core of a magnetic vortex in a square array of nanodots has been experimentally detected. The appearance of a frequency multiplet has been theoretically explained. It has been shown that a reason for the lift of degeneracy can be the magnetostatic interaction between nanodots.

DOI: 10.1134/S0021364015080068

Two-dimensional (2D) arrays of nanodots with different shapes attract great attention in view of prospects of their use in spintronic devices for various aims. The shapes and dimensions nanoparticles composing film arrays are very diverse. However, they are usually cylinders with a height of several tens of nanometers and a width of tens of nanometers to several microns. It is known that, at certain relations between the thickness of a nanodot and its width (diameter), a stable distribution of the magnetization occurs in the form of a vortex with a Bloch point in the center of a magnet. The static and dynamic magnetic properties of individual circular nanodots are quite well studied theoretically: the theory describing the dynamics of the magnetization was developed on the basis of the Thiele equation (in terms of collective variables [1, 2]) and it was shown that the core of the magnetic vortex executes gyrotropic motion around the axis of a nanodisk similar to the Larmor motion of a charged particle around the magnetic field lines. The angular velocity of this motion of the vortex core is relatively low (<1 GHz). The inclusion of the inertia of the magnetic vortex and the third-order gyrotropic factor made it possible to predict and, then, to detect the existence of a high-frequency doublet (at frequencies of about several gigahertz) and to demonstrate the presence of a “fine structure” on the trajectory of the core [3–6].

Experimental tools for studying nanodots are also widely developed (see, e.g., [7, 8]). The cited works present the results of experimental studies of the magnetic properties of individual nanodots. These results confirm the theoretically predicted frequency of gyrotropic motion of the core and the linear dependence of

this frequency on the magnetic field perpendicular to the plane of the nanodot. The mechanism of dynamic remagnetization of the nanodot was analyzed. However, most experiments deal with films, i.e., arrays of fairly separated nanodots. For this reason, the interaction between magnetic subsystems of elements of an array is usually disregarded [9]. At the same time, the long-term magnetostatic interaction can affect at least collective modes of rotational motion of the core if not the static or quasistatic characteristics of the magnetization [10–14]. Understanding of the character of collective motion of cores in arrays where the distances between nanodots are comparable or slightly larger than the dimensions of elements themselves is particularly important. Even a stronger exchange interaction between magnetizations [15], which is due to the existence of magnetic “bridges” between neighboring elements of the array, was revealed in practically dense packed arrays. Multiplets at frequencies at which isolated nanodots exhibit splitting were observed in ferromagnetic resonance (FMR) experiments because of interaction.

A similar effect should also apparently be expected in the case of a weaker but long-range magnetostatic interaction. Among the works on the dynamic characteristics of interacting nanodots, we specially point to work [16], where the problem of vibrational modes of a pair of coaxially arranged, magnetostatically interacting nanodisks was analytically solved.

The array of circular nanodots for our studies was formed by the Lif-off method from a continuous film by thermal sputtering from the 80HXC alloy on a silicon substitute. The dimensions of the array were 4 × 4 mm. The thickness of a pattern film and its compo-

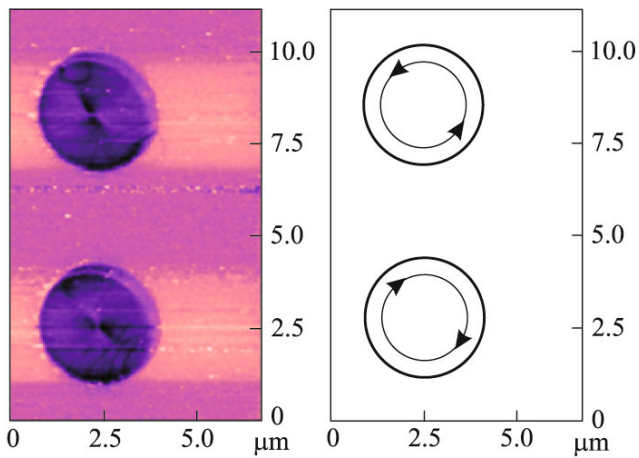


Fig. 1. (Color online) (Left panel) Photograph of the structure the magnetization of circular nanodots and (right panel) the corresponding schematic of the direction of the magnetization.

sition were determined by X-ray fluorescence analysis. The thickness of nanodots in the resulting array was $L = 104$ nm, the radius was $R = 1.6$ μm , and the distance was $4R$ between the centers of two neighboring nanodots. The saturation magnetization of the material was determined on an ELEXSYS E580 EPR spectrometer. It corresponded to a value of 770 G.

The magnetic properties were examined by means of the longitudinal magneto-optic Kerr effect at a NanoMOKE 2 setup. A sample was placed in the focal plane of the optical system. The diameter of the laser beam with the wavelength $\lambda = 630$ nm was $d = 30$ μm . Remagnetization was performed at a frequency of 27 Hz in the field applied in the plane of the film.

The morphology of the surface and the magnetic relief were studied on a Veeco MultiMode NanoScope IIIa SPM System scanning probe microscope. The chirality direction $q = \pm$ on images was determined from the distribution of the gradient of magnetic forces acting on the probe of the cantilever (Fig. 1). The sign of the parameter q is determined by the direction of the magnetization of the vortex (clockwise or counterclockwise). Figure 2 shows the photograph of the array of nanospots after the FMR spectrometer experiment. It is seen that the spots have both positive and negative chirality.

The magnetic resonance properties of the array of nanodots were studied on an FMR spectrometer at a frequency of 232 MHz. The sample was placed in the antinode of the magnetic field of a cavity, which was a short-circuited quarter-wave waveguide with a 4-mm-wide central strip. The amplitude of the alternating magnetic field parallel to the plane of the film was ≈ 1 Oe. The static magnetic field was perpendicular to the plane of the waveguide (main field). A signal from the sample was amplified by a selective amplifier at a modulation frequency of ≈ 1 kHz and was supplied to a synchronous detector. The main field in the experi-

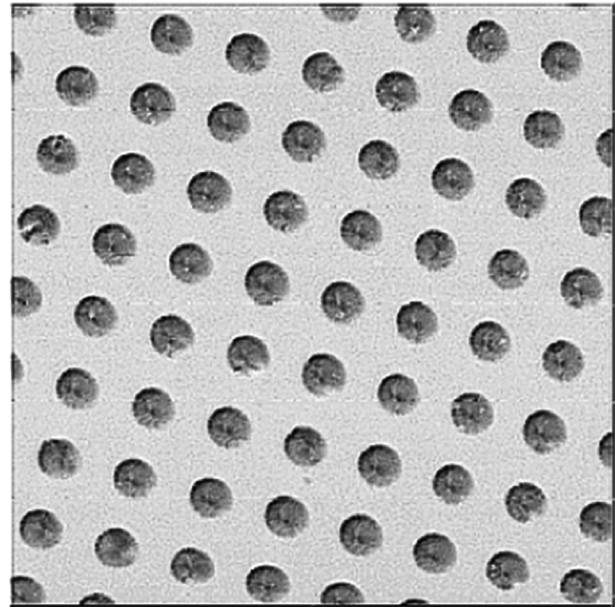


Fig. 2. Photograph of the array of nanodots. The distribution of the contrast of color of disks makes it possible to reveal the direction of the chirality q .

ment was perpendicular to the surface of the film and was varied from -5 to 5 kOe. Negative values correspond to the field opposite to the conditional vector normal to the surface of the film. As a result, we obtained the differential dependences of the absorbance of the sample on the main field. Their characteristic form is shown in Fig. 3. It is important that nanodots with the polarity opposite to the main field are responsible for the resonance regime in this case, because resonance in the sample under study can occur at frequencies below 300 MHz only in this case (see, e.g., [8–10]). At the same time, resonance was detected in both the positive and the negative range of

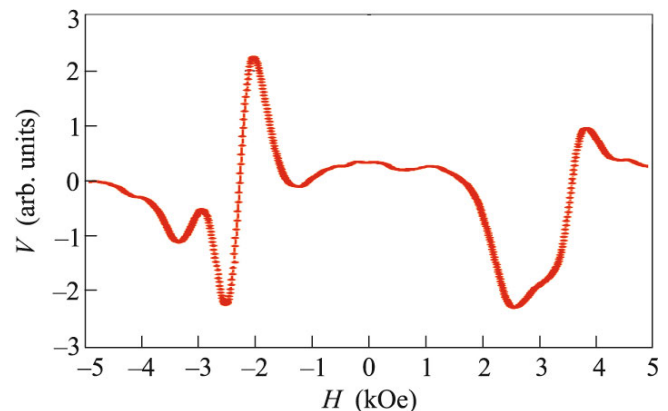


Fig. 3. Differential absorption curves obtained in the FMR experiment on the array of nanodots. The nonmonotonicity of absorption curves indicates a superposition of resonance curves with slightly different frequencies.

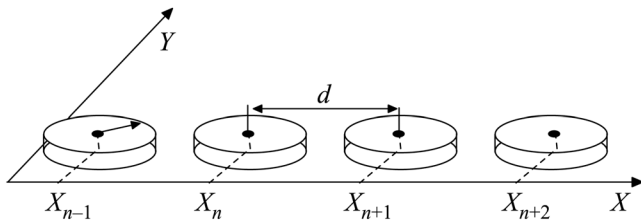


Fig. 4. Model of a one-dimensional chain of nanodisks.

the main field. This indicates that disks where the magnetization in cores is opposite to the field inevitably exist in the film at any direction of the main field. The absorption curves in Fig. 3 have the form of a superposition of no less than two curves with different absorption widths and resonance frequencies. This means the splitting of the resonance frequency of the gyrotropic motion of vortices. We attribute this effect to the existence of a weak but long-range magnetostatic interaction between nanodisks.

We theoretically consider a model situation that can qualitatively explain the reason for the lift of the degeneracy of the resonance frequency. The number of elements in real films (arrays of nanodisks) is very large, and the effect of each disk on any other disk should be taken into account when describing the collective motion of the magnetization. As a result, the analytical calculation of collective modes is significantly complicated. For this reason, we consider in this work a simplified model—a part of the two-dimensional array. This is a chain of linearly arranged nanodisks with alternating parameters of the magnetization. In spite of the simplicity of the model, this system makes it possible to understand some dynamical properties of arrays of interacting particles.

We first consider a one-dimensional chain of nanodots in the form of circular cylinders whose centers are located at the same distance d from each other (see Fig. 4). It is known that one of the equilibrium distributions of the magnetization in circular nanocylinders is a vortex structure [17–21] where the magnetization leaves the plane of the magnet in the center of the vortex and a core appears. Below, we use an approximation in which the profile of the magnetization of the vortex hardly changes at the displacement of the core from the center (rigid magnetic vortex model). The behavior of the core in alternating magnetic fields with relatively low frequencies (≤ 1 GHz) is similar to the gyrotropic motion of a quasiparticle. When the effective mass of the magnetic subsystem, third-order gyrovector, and damping are neglected, the behavior of the core is described by the equation of motion in the form

$$\mathbf{G} \times \mathbf{v} - \nabla U + \mathbf{F} = 0. \quad (1)$$

Here, \mathbf{G} is the gyrovector, \mathbf{v} is the velocity of the core of the magnetic vortex, U is the potential energy of the magnetization (its change at the displacement of the

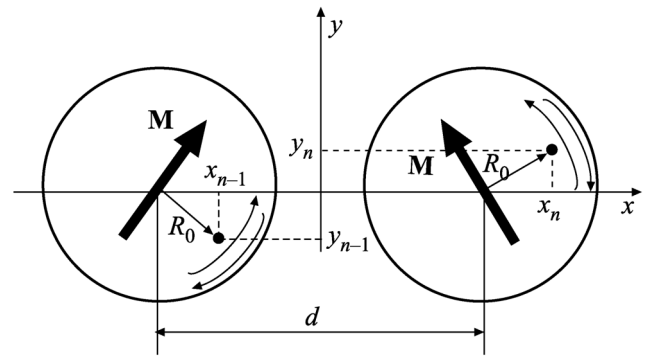


Fig. 5. Coordinate system and the scheme of the magnetostatic interaction between disks. Circles indicate the positions of the vortex core and thick arrows show the directions of the magnetic moment. The clockwise direction of the magnetization is chosen on both disks. Thin arrows near the edges of the disks indicate the possible directions of motion of the core.

core from the center of the spot is usually attributed to an increase in the magnetostatic energy), and \mathbf{F} is the force with which neighboring nanodisks act on the vortex core (as on a quasiparticle). According to Eq. (1), the vortex core is involved in a complex motion in the presence of a gyroscopic force [22–27]. Equation (1) for a single magnet was first proposed by Thiele [1] and was obtained from the Landau–Lifshitz equation at the passage to collective variables.

We supplement this equation with the force \mathbf{F} that appears owing to the magnetostatic interactions between cylinders. It is assumed that this interaction very weakly affects the dynamic characteristics of the array of nanodots. This assumption is justified in the case of a large distance between dots: $d \gg R$. In other cases, it should be expected that magnetic subsystems of at least neighboring cylinders affect each other.

We consider the mechanism of the magnetostatic interaction by an example of two neighboring disks. Figure 5 shows the direction of the magnetic moment \mathbf{M} at the displacement of the core from the center of the nanodot. It was shown in [28] that the configuration of the magnetic field beyond the nanodot is similar to the configuration of the field of a magnetic dipole. Consequently, the dipole approximation can be used below to estimate the energy of interaction between cylinders. It is noteworthy that the magnitude of the magnetic moment \mathbf{M} is determined by the displacement of the core from the equilibrium position, which in turn depends not only on the field applied along the plane of the cylinder but also on the frequency of its variation. Indeed, in the case of resonance motion, the radius of the trajectory of the vortex is quite large (comparable with the radius of the cylinder itself) even at small amplitudes of the field. In the general case, $|\mathbf{M}| = M(h, \omega_h)$, where $h = H/H_s$ is the dimensionless amplitude of the magnetic field (divided by the saturation field) and ω_h is the cyclic frequency of the varia-

tion of the magnetic field. We note that the contribution to the dipole moment of the disk from the core itself is small because of its small volume. For this reason, we neglect this factor in this work. In contrast, the model of “hard” vortex can be inapplicable in the case of large diameters of the disks. In this case, magnetic charges are hardly induced on the lateral surface of disks and the contribution of the magnetic moments of cores to the energy of interaction between disks can be significant. A detailed analytical calculation of collective modes in the model with the interaction between the magnetizations of only identically oriented cores was performed in [29].

In the approximation of a parabolic potential well U for the returning force acting on the vortex core, $\nabla U = \kappa \mathbf{r}$, where κ is the so-called effective stiffness of the magnetic subsystem. In this case, Eq. (1) has the form

$$\mathbf{G} \times \mathbf{v} - \kappa \mathbf{r} + \mathbf{F} = 0. \quad (2)$$

In the projections on the coordinate axes, the equation for the n th disk has the form

$$\begin{aligned} G\dot{y}_n - \kappa x_n + F_{x_n} &= 0, \\ -G\dot{x}_n - \kappa y_n + F_{y_n} &= 0. \end{aligned} \quad (3)$$

We estimate the force F . In the dipole approximation, the energy of magnetostatic interaction between disks spaced from each other by m periods can be represented in the form

$$\begin{aligned} W_{n-m} \\ = [\mathbf{M}_{n-m} \mathbf{M}_n - 3(\mathbf{M}_{n-m} d)(\mathbf{M}_n d)/(md)^2]/(md)^3. \end{aligned}$$

This energy can be represented in the form of a function of the coordinates of the vortex core (see Fig. 5):

$$\begin{aligned} W_{n-m} &= \frac{q_n q_{n-m} M^2}{(md)^3} [\cos(\phi_{n-m}) \cos(\phi_n) \\ &\quad - 2 \sin(\phi_{n-m}) \sin(\phi_n)] \\ &= \frac{q_n q_{n-m} M^2}{(md)^3 R_0^2} (x_{n-m} x_n - 2y_{n-m} y_n). \end{aligned} \quad (4)$$

Here, R_0 is the rms radius of the trajectory of the vortex core. The angles ϕ are measured from the x axis. It is important that the direction of the effective magnetic moment of disks at the displacement of the core and, therefore, the sign of the contribution of the magnetostatic energy as a function of the coordinates of the core depend on the sign of the chirality q . In view of Eq. (4), the effective force acting on the core by the other disks of the system is given by the expressions

$$\begin{aligned} F_{x_n} &= -\frac{\partial}{\partial x_n} \sum_{n \neq m} (W_{n-m} + W_{n+m}) \\ &= -\frac{q_n M^2}{d^3 R_0^2} \sum_{n \neq m} \frac{1}{m^3} (q_{n-m} x_{n-m} + q_{n+m} x_{n+m}), \end{aligned} \quad (5)$$

$$\begin{aligned} F_{y_n} &= -\frac{\partial}{\partial y_n} \sum_{n \neq m} (W_{n-m} + W_{n+m}) \\ &= \frac{q_n M^2}{d^3 R_0^2} \sum_{n \neq m} \frac{1}{m^3} (q_{n-m} y_{n-m} + q_{n+m} y_{n+m}). \end{aligned} \quad (6)$$

Taking into account Eqs. (5) and (6), we represent the system of equations (3) in the form

$$\begin{aligned} G\dot{y}_n - \kappa x_n - \varepsilon q_n \sum_{n \neq m} \frac{1}{m^3} (q_{n-m} x_{n-m} \\ + q_{n+m} x_{n+m}) &= 0, \\ -G\dot{x}_n - \kappa y_n - 2\varepsilon q_n \sum_{n \neq m} \frac{1}{m^3} (q_{n-m} y_{n-m} \\ + q_{n+m} y_{n+m}) &= 0, \\ \varepsilon &= \frac{M^2}{d^3 R_0^2}. \end{aligned} \quad (7)$$

The solution of system (7) can be represented in the form $x_n = a_n \cos(kX_n - q_n p_n \omega t)$, $y_n = b_n \sin(kX_n - q_n p_n \omega t)$. Here, $p = \pm 1$ is the polarity of the vortex corresponding to the direction of the magnetization in the center of the core, X_n is the coordinate of the center of the nanodot, k is the wavenumber, and the product $q_n p_n$ determines the direction of the precession of the n th vortex core (clockwise or counterclockwise). We consider the following distribution of the parameters p and q of disks. Let the disks with odd numbers have chirality q and polarity p and the disks with even numbers have chirality q' and polarity p' . The substitution of trial solutions into Eqs. (7) for a pair of neighboring disks, which is an element of the chain, gives

$$\begin{aligned} Gb\omega qp + [\kappa + 2\varepsilon S_e(k)]a + 2\varepsilon qq'a'S_0(k) &= 0, \\ Ga\omega qp + [\kappa - 4\varepsilon S_e(k)]b - 4\varepsilon pp'b'S_0(k) &= 0, \\ G'b'\omega q'p' + [\kappa + 2\varepsilon S_e(k)]a' + 2\varepsilon qq'a'S_0(k) &= 0, \\ G'a'\omega q'p' + [\kappa - 4\varepsilon S_e(k)]b' + 2\varepsilon pp'b'S_0(k) &= 0. \end{aligned} \quad (8)$$

Here,

$$S_e(k) = \sum_{m=1,3,5,\dots} [\cos(mkd)/m^3],$$

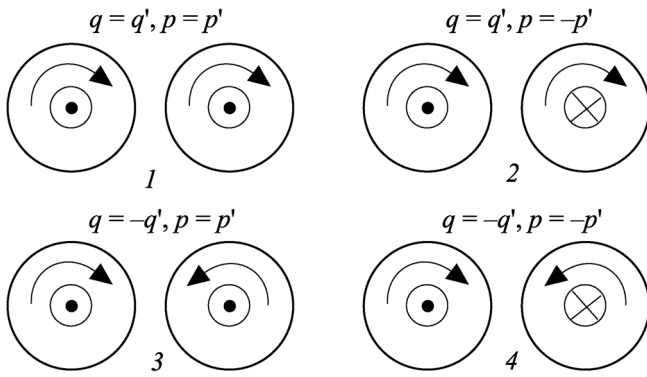


Fig. 6. Possible combination of chirality and polarity in an element of a one-dimensional chain of nanodisks.

$$S_0(k) = \sum_{m=2,4,6,\dots} [\cos(mkd)/m^3].$$

The parameters G , G' , and κ have the form [8, 27]

$$\begin{aligned} G &= qp \frac{2\pi M_S L}{\gamma} (1 - ph), \\ G' &= q'p' \frac{2\pi M_S L}{\gamma} (1 - p'h), \\ \kappa &= \frac{40\pi M_S^2 L^2}{9R} (1 - h^2), \end{aligned} \quad (9)$$

where L is the thickness of the nanodisk, γ is the gyromagnetic ratio, and h is the dimensionless field perpendicular to the plane of disks.

The condition of zero determinant of the matrix constructed from the coefficients of the parameters a , b , a' , and b' in Eqs. (8) provides a biquadratic equation for the unknown ω . The solution for resonance modes has the form

$$\omega^2 = -\frac{B}{2A} \mp \sqrt{\left(\frac{B}{2A}\right)^2 - \frac{C}{A}}, \quad (10)$$

where

$$\begin{aligned} A &= G^2 G'^2, \\ B &= -(G^2 + G'^2)[\kappa^2 - 2\kappa\epsilon S_e(k) - 8\epsilon^2 S_e^2(k)] \\ &\quad + 16GG'\epsilon^2 S_0^2(k), \\ C &= \kappa^4 - 4\kappa^3\epsilon S_e(k) - 36\kappa^2\epsilon^2 S_0^2(k). \end{aligned} \quad (11)$$

In the limit $d \gg R$, when the interaction between disks is absent, Eq. (10) gives the well-known result for the frequency of gyrotropic motion of the core in the isolated disk: $\Omega_0 = \kappa/G$ and $\Omega'_0 = \kappa/G'$.

The possible configurations of chains of alternating disks are shown in Fig. 6. For various combinations of the parameters q , q' , p , and p' , there are four scenarios

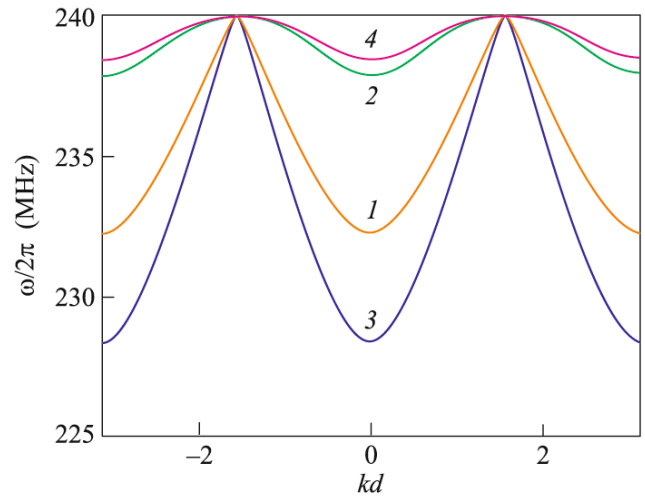


Fig. 7. (Color online) Dispersion relations (10) in the presence of the main magnetic field $h = -0.25$ perpendicular to the plane of the film, which approximately corresponds to resonance (see Fig. 3). The curves are plotted with the parameters of a permalloy disk: $M_S = 770$ Oe, $L = 104$ nm, and $R = 1.6$ μm . It is assumed that $R_0 \approx R$ and, therefore, $M \approx M_S V$ (V is the volume of the disk) near the resonance state. The enumeration of the curves corresponds to the combinations of q and p presented in Fig. 6.

of collective rotations of cores with corresponding dispersion relations (10). Figure 7 shows the characteristic form of dispersion curves demonstrating the splitting of the frequency. The existence of a multiplet in zero external field was predicted in [30] and was partially confirmed in the experiment [28], but the system of only two or four interacting disks was considered in those works.

We note that alternations of p and q shown in Fig. 6 are not the only possible variants in chains of a large number of disks. Indeed, more complex variants with several successive disks with identical p and/or q values or any other combinations are possible. However, only the examined distribution of the parameters p and q gives the maximum splitting of the resonance frequency.

It is worth noting that we did not observe the strict alternation of p and q values in the films under study. Disks with identical polarities and chiralities form islands consisting of several particles. However, we believe that the splitting of the frequency in this case insignificantly differs from our estimate (10).

To conclude, the presence of closely located absorption peaks can be attributed to the lift of the degeneracy of the resonance frequency because of the effect of the magnetostatic interaction between disks.

According to Eq. (10), closely located absorption peaks should be observed near the resonance state. They coincide on the curves in Fig. 3; as a result, non-monotonocities and bends appear. The maximum splitting calculated by Eq. (10) in the long-wavelength

limit is $\Delta h \approx 0.06$. It is in satisfactory agreement with experimental data shown in Fig. 3.

We are grateful to V.Ya. Prints for assistance in the fabrication of arrays of quantum dots. This work was supported by the Russian Science Foundation (project no. 14-15-00805 “Biofunctional Magnetic-Vortex Nanodisks Modified by DNA Aptamers for Targeted Microsurgery of Malignant Neoplasms” for 2014–2016).

REFERENCES

1. A. A. Thiel, Phys. Rev. Lett. **30**, 230 (1975).
2. J. Kim and S.-B. Choe, J. Magn. **12**, 113 (2007).
3. F. G. Mertens, H. J. Schnitzer, and A. R. Bishop, arXiv:cond-mat/9902151v1 (1999).
4. F. G. Mertens and A. R. Bishop, arXiv:cond-mat/9903037v1 (1999).
5. B. A. Ivanov and D. D. Sheka, JETP Lett. **82**, 436 (2005).
6. B. A. Ivanov, G. G. Avanesyan, A. V. Khval'kovskii, N. E. Kulagin, K. E. Zaspel, and K. A. Zvezdin, JETP Lett. **91**, 178 (2010).
7. B. Pigeau, G. de Loubens, O. Klein, A. Riegler, F. Lochner, G. Schmidt, L. W. Molenkamp, V. S. Tiberkevich, and A. N. Slavin, Appl. Phys. Lett. **96**, 132506 (2010).
8. G. Loubens, A. Riegler, B. Pigeau, F. Lochner, F. Boust, K. Y. Guslienko, H. Hurdequint, L. W. Molekamp, G. Schmidt, A. N. Slavin, S. Tiberkevich, N. Vukadinovic, and O. Klein, Phys. Rev. Lett. **B 102**, 177602 (2009).
9. V. Novosad, F. Y. Fradin, P. E. Roy, K. S. Buchanan, K. Yu. Guslienko, and S. D. Bader, Phys. Rev. B **72**, 024455 (2005).
10. V. A. Orlov and P. D. Kim, J. Sib. Fed. Univ. Math. Phys. **6**, 86 (2013).
11. V. S. Prokopenko, P. D. Kim, V. A. Orlov, B. V. Vasiliev, D. K. Vovk, S. E. Zatsupilin, and R. Yu. Rudenko, J. Sib. Fed. Univ. Math. Phys. **6**, 262 (2013).
12. P. D. Kim, V. A. Orlov, V. S. Prokopenko, S. S. Zamai, V. Ya. Prints, R. Yu. Rudenko, and T. V. Rudenko, Phys. Solid State **57**, 30 (2015).
13. Yu. P. Ivanov, E. V. Pustovalov, A. V. Ognev, and L. A. Chebotkevich, Phys. Solid State **51**, 2300 (2009).
14. K. Yu. Guslienko, V. Novosad, Y. Otani, H. Shima, and K. Fukamichi, Phys. Rev. B **65**, 024414 (2001).
15. J. Dou, S. C. Hernandez, C. Yu, M. J. Pechan, L. Folks, J. A. Katine, and M. J. Carey, J. Appl. Phys. **107**, 09B514 (2010).
16. S. S. Cherepov, B. C. Koop, V. Korenivski, D. C. Worledge, A. Yu. Galkin, R. S. Khymyn, and B. A. Ivanov, Phys. Rev. Lett. **109**, 097204 (2012).
17. J. Miltat and A. Thiaville, Science **298**, 555 (2002).
18. A. Puzic, B. Van Waeyenberge, K. W. Chou, P. Fischer, H. Stoll, G. Schutz, T. Tylliszczak, K. Rott, H. Bruckl, G. Reiss, I. Neudecker, Th. Haug, M. Buess, and C. H. Back, J. Appl. Phys. **97**, 10E704 (2005).
19. T. Shinjo, T. Okuno, R. Hassdorf, K. Shigeto, and T. Ono, Science **289**, 930 (2000).
20. J. Raabe, R. Pulwey, R. Sattler, T. Schweinbock, J. Zweck, and D. Weiss, J. Appl. Phys. **88**, 4437 (2000).
21. B. A. Ivanov and D. D. Sheka, J. Low Temp. Phys. **21**, 881 (1995).
22. O. Klein, G. de Loubens, V. V. Naletov, F. Boust, T. Guillet, H. Hurdequint, A. Leksikov, A. N. Slavin, V. S. Tiberkevich, and N. Vukadinovic, Phys. Rev. B **78**, 144410 (2008).
23. K.-S. Lee and S.-K. Kim, Appl. Phys. Lett. **91**, 132511 (2007).
24. V. P. Kravchuk, Yu. Gaididei, and D. D. Sheka, Phys. Rev. B **80**, 100405(R) (2009).
25. K.-S. Lee, K. Yu. Guslienko, J.-Y. Lee, and S.-K. Kim, Phys. Rev. B **76**, 174410 (2007).
26. B. A. Ivanov and G. M. Wysin, Phys. Rev. B **65**, 134434 (2002).
27. K. Yu. Guslienko, B. A. Ivanov, V. Novosad, Y. Otani, H. Shima, and K. Fukamichi, J. Appl. Phys. **91**, 8037 (2002).
28. A. Vogel, A. Drews, T. Kamionka, M. Bolte, and G. Meier, Phys. Rev. Lett. **105**, 037201 (2010).
29. A. Yu. Galkin and B. A. Ivanov, J. Exp. Theor. Phys. **109**, 74 (2009).
30. J. Shibata, K. Shigeto, and Y. Otani, Phys. Rev. B **67**, 224404 (2003).

Translated by R. Tyapaev